Geochemical constraints on the use of an amorphous precursor phase by corals

G.L. Foster, D. Evans

Supplementary Information

The Supplementary Information includes:

- Rayleigh Distillation Model Description
- Data Sources Used to Perform the Calculations
- Model Code
- Table S-1
- Figures S-1 and S-2
- Supplementary Information References

Rayleigh Distillation Model Description

The model presented in the main text can be represented algebraically as follows. The Rayleigh distillation equation for the final aragonite precipitation step is written as:

$$D = (1 - f_{Ca}^{\alpha})/(1 - f_{Ca}) \quad \text{(Eq. S-1)}$$

where D is the 'apparent' distribution coefficient of the biomineral relative to seawater, f_{Ca} is the fraction Ca utilised, and α is the open system inorganic distribution coefficient. To include an ACC precursor step, the equation must be modified to account for the dissolution-reprecipitation of ACC. This is principally because calcium is greatly concentrated in solid phases, which means that the delivery of minor amounts of ACC to the calcifying space could greatly increase the seawater $[Ca^{2+}]$ once it is dissolved (e.g. 1 mg of ACC dissolved in 1 ml of seawater would result in an approximately doubled $[Ca^{2+}]$). To our knowledge, there are no constraints on the rate at which ACC is delivered to the calcifying space in organisms that utilise this pathway. As such, we modify Eq. S-1 to include the calcification site ACC/seawater ratio as an unknown, which allows the resulting apparent distribution coefficients in biogenic aragonite to be modelled as a function of both this ratio and the fraction Ca utilised in the subsequent calcite precipitation:

$$D = (1 - f_{Ca}^{\alpha})/(1 - f_{Ca}) \cdot (X/Ca_{ECF})/(X/Ca_{SW}) \quad \text{(Eq. S-2)}$$

where X/Ca_{ECF} and X/Ca_{SW} are the molar trace element/Ca ratios at the calcification site and in seawater respectively. The element/Ca ratio of the calcification site can be calculated by determining the degree to which the trace element concentration is modified by ACC delivery, by multiplying the molar ACC element/Ca ratio by the amount of ACC delivered, and adding this to the existing concentration from seawater transport, by expanding as follows:

$$D = (1 - f_{Ca}^{\alpha})/(1 - f_{Ca}) \cdot (([TE_{SW}]+rACC\text{-}sw \cdot D_{ACC} \cdot X/Ca_{sw})/[Ca_{ECF}])/(X/Ca_{SW}) \quad \text{(Eq. S-3)}$$

where $[TE_{SW}]$ is the trace element concentration in seawater, rACC-sw is the ratio of ACC/seawater in the calcifying space, D_{ACC} are the empirically derived ACC trace element distribution coefficients (derived from inorganic precipitation experiments), X/Ca_{sw} is the molar trace element/Ca ratio in seawater, and $[Ca_{ECF}]$ is the calcification site $[Ca^{2+}]$. Because we model this as a two-stage process, two Rayleigh distillation models must be produced, one for the aragonite precipitation step (Eq. S-1), and one for the ACC precipitation step. As such, D_{ACC} in Eq. S-3 modifies the ACC values given by Evans *et al.* (2020) as follows:

$$D_{ACC} = (1 - f_{Ca}^{\beta})/(1 - f_{Ca}) \quad \text{(Eq. S-4)}$$

where β are the empirical ACC distribution coefficients. We use $f_{Ca} = 0$ for the ACC precipitation step for simplicity in the absence of any information regarding its likely value, and note that this choice has no material impact on our results (see Fig. S-1). Combining Eqs. S-3 and S-4 gives predicted apparent distribution coefficients for biogenic aragonite in three-dimensional $f_{Ca\text{-}aragonite}$-$f_{Ca\text{-}ACC}$-rACC-sw space where $f_{Ca\text{-}aragonite}$ and $f_{Ca\text{-}ACC}$ are the fraction Ca utilisation during the aragonite and ACC precipitation step respectively.

ACC dissolution is likely to take place only up to certain ACC/seawater ('water/rock') ratios because beyond a certain point, partial ACC dissolution will result in a calcification site oversaturated with respect to the remaining solid phase, which would then be stabilised. We do not know that solubility of biogenic ACC, but by analogy to inorganically precipitated ACC from seawater, seawater becomes oversaturated with respect to ACC at $[Ca^{2+}][CO_3^{2-}]$ products of ~100 mM^2 (Evans *et al.*, 2019). For this reason, we smoothly transition between complete ACC dissolution-reprecipitation at (and below) ACC/seawater = 10^0 mg/ml (equivalent to an ECF $[CO_3^{2-}]$ approaching 10 mM) and complete solid state crystallisation, i.e., no cation exchange with the ECF, at ACC/seawater = 10^1 mg/ml. While this latter choice is arbitrary, the threshold for the point at which only solid state crystallisation occurs impacts our results only in expanding or shrinking the portion of the parameter space with ACC/seawater $>10^0$ mg/ml.

Data Sources Used to Perform the Calculations

The data reported in the supplementary table and displayed in main text Fig. 4A,B can be found in the following references: (Allison and Finch, 2004, 2007; Allison *et al.*, 2005; Brahmi *et al.*, 2012; Case *et al.*, 2010; Chen *et al.*, 2022; Cohen *et al.*, 2001; Cuif and Dauphin, 1998; Fietzke and Wall, 2022; Gagnon *et al.*, 2007; Jurikova *et al.*, 2019; Meibom *et al.*, 2004, 2006; Rollion-Bard and Blamart, 2015; Schleinkofer *et al.*, 2019; Sinclair and Risk, 2006; Standish *et al.*, 2024).

The model described above uses inorganic aragonite trace element distribution coefficient data from the following references: (Castillo Alvarez *et al.*, 2025; Füger *et al.*, 2019; Gaetani and Cohen, 2006; Gvirtzman *et al.*, 1973; Holcomb *et al.*, 2016; Okumura and Kitano, 1986; Raiswell and Brimblecombe, 1977).

Model Code

The model code (.mlx) is available for download from the online version of this article at https://doi.org/10.7185/geochemlet.2623.

Supplementary Table

Table S-1 A compilation of coral skeletal data used to compare to our model results.

Table S-1 (.xlsx) is available for download from the online version of this article at https://doi.org/10.7185/geochemlet.2623.

Supplementary Figures

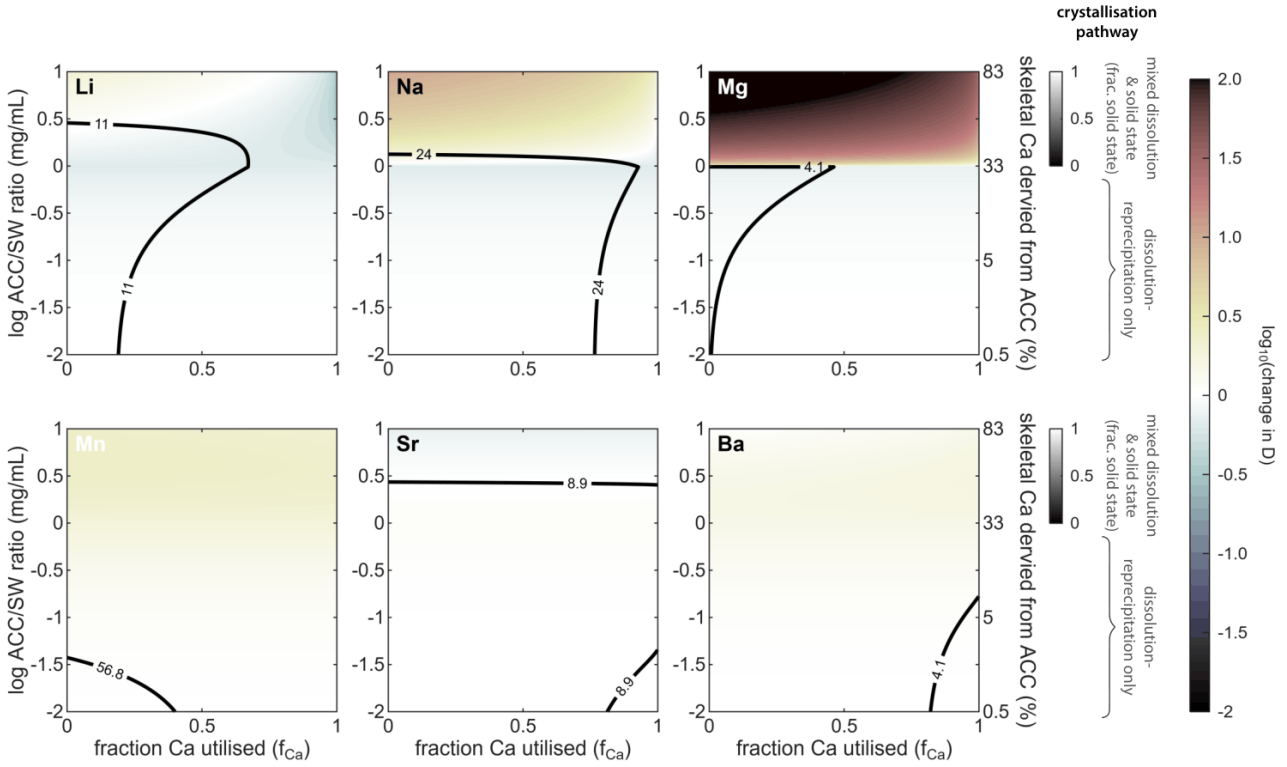

Figure S-1 As main text Fig. 3, except assuming $f_{Ca} = 0.5$ rather than $f_{Ca} = 0$ during the ACC precipitation step.

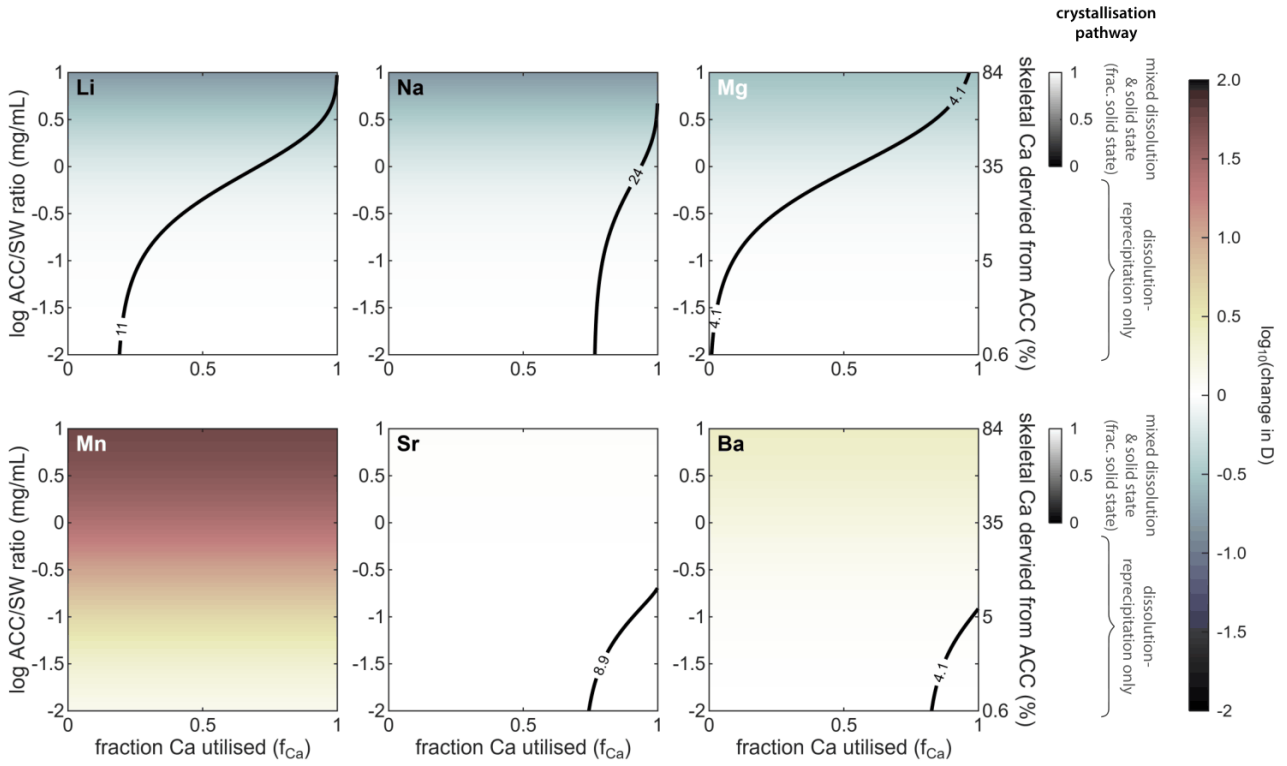

Figure S-2 As main text Fig. 3, except alternatively assuming that ACC undergoes complete dissolution-reprecipitation at all ACC/seawater ratios (our preferred model discussed in the main text switches to solid state transformation above 10^0 mg/ml ACC/seawater). All trace element systems except Mn remain insensitive to ACC delivery up to substantial degrees of ACC transport (~10^0 mg/ml).

Supplementary Information References

Allison, N., Finch, A.A. (2004) High-resolution Sr/Ca records in modern *Porites lobata* corals: Effects of skeletal extension rate and architecture. *Geochemistry, Geophysics, Geosystems* 5, Q05001. https://doi.org/10.1029/2004GC000696

Allison, N., Finch, A.A. (2007) High temporal resolution Mg/Ca and Ba/Ca records in modern *Porites lobata* corals. *Geochemistry, Geophysics, Geosystems* 8, Q05001. https://doi.org/10.1029/2006GC001477

Allison, N., Finch, A.A., Newville, M., Sutton, S.R. (2005) Strontium in coral aragonite: 3. Sr coordination and geochemistry in relation to skeletal architecture. *Geochimica et Cosmochimica Acta* 69, 3801–3811. https://doi.org/10.1016/j.gca.2005.01.026

Brahmi, C., Kopp, C., Domart-Coulon, I., Stolarski, J., Meibom, A. (2012) Skeletal growth dynamics linked to trace-element composition in the scleractinian coral *Pocillopora damicornis*. *Geochimica et Cosmochimica Acta* 99, 146–158. https://doi.org/10.1016/j.gca.2012.09.031

Case, D.H., Robinson, L.F., Auro, M.E., Gagnon, A.C. (2010) Environmental and biological controls on Mg and Li in deep-sea scleractinian corals. *Earth and Planetary Science Letters* 300, 215–225. https://doi.org/10.1016/j.epsl.2010.09.029

Castillo Alvarez, C., Hathorne, E., Clog, M., Finch, A., Kröger, R., Penkman, K., Allison, N. (2025) Aragonite lithium/magnesium as an indicator of calcification media saturation state in marine calcifiers. *Communications Earth & Environment* 6, 984. https://doi.org/10.1038/s43247-025-02945-3

Chen, Y., Zhai, F., Li, P., Gu, Y., Wu, K. (2022) Extreme 2020 Summer SSTs in the Northern South China Sea: Implications for the Beibu Gulf Coral Bleaching. *Journal of Climate* 35, 4177–4190. https://doi.org/10.1175/JCLI-D-21-0649.1

Cohen, A.L., Layne, G.D., Hart, S.R., Lobel, P.S. (2001) Kinetic control of skeletal Sr/Ca in a symbiotic coral: Implications for the paleotemperature proxy. *Paleoceanography* 16, 20–26. https://doi.org/10.1029/1999PA000478

Cuif, J.-P., Dauphin, Y. (1998) Microstructural and physico-chemical characterization of 'centers of calcification' in septa of some Recent scleractinian corals. *Paläontologische Zeitschrift* 72, 257–269. https://doi.org/10.1007/BF02988357

Evans, D., Webb, P.B., Penkman, K., Kröger, R., Allison, N. (2019) The Characteristics and Biological Relevance of Inorganic Amorphous Calcium Carbonate (ACC) Precipitated from Seawater. *Crystal Growth & Design* 19, 4300–4313. https://doi.org/10.1021/acs.cgd.9b00003

Evans, D., Gray, W.R., Rae, J.W.B., Greenop, R., Webb, P.B., Penkman, K., Kröger, R., Allison, N. (2020) Trace and major element incorporation into amorphous calcium carbonate (ACC) precipitated from seawater. *Geochimica et Cosmochimica Acta* 290, 293–311. https://doi.org/10.1016/j.gca.2020.08.034

Fietzke, J., Wall, M. (2022) Distinct fine-scale variations in calcification control revealed by high-resolution 2D boron laser images in the cold-water coral *Lophelia pertusa*. *Science Advances* 8, eabj4172. https://doi.org/10.1126/sciadv.abj4172

Füger, A., Konrad, F., Leis, A., Dietzel, M., Mavromatis, V. (2019) Effect of growth rate and pH on lithium incorporation in calcite. *Geochimica et Cosmochimica Acta* 248, 14–24. https://doi.org/10.1016/j.gca.2018.12.040

Gaetani, G.A., Cohen, A.L. (2006) Element partitioning during precipitation of aragonite from seawater: A framework for understanding paleoproxies. *Geochimica et Cosmochimica Acta* 70, 4617–4634. https://doi.org/10.1016/j.gca.2006.07.008

Gagnon, A.C., Adkins, J.F., Fernandez, D.P., Robinson, L.F. (2007) Sr/Ca and Mg/Ca vital effects correlated with skeletal architecture in a scleractinian deep-sea coral and the role of Rayleigh fractionation. *Earth and Planetary Science Letters* 261, 280–295. https://doi.org/10.1016/j.epsl.2007.07.013

Gvirtzman, G., Friedman, G.M., Miller, D.S. (1973) Control and distribution of uranium in coral reefs during diagenesis. *Journal of Sedimentary Research* 43, 985–997. https://doi.org/10.1306/74D728CE-2B21-11D7-8648000102C1865D

Holcomb, M., DeCarlo, T.M., Gaetani, G.A., McCulloch, M. (2016) Factors affecting B/Ca ratios in synthetic aragonite. *Chemical Geology* 437, 67–76. https://doi.org/10.1016/j.chemgeo.2016.05.007

Jurikova, H., Liebetrau, V., Raddatz, J., Fietzke, J., Trotter, J., Rocholl, A., Krause, S., McCulloch, M., Rüggeberg, A., Eisenhauer, A. (2019) Boron isotope composition of the cold-water coral *Lophelia pertusa* along the Norwegian margin: Zooming into a potential pH-proxy by combining bulk and high-resolution approaches. *Chemical Geology* 513, 143–152. https://doi.org/10.1016/j.chemgeo.2019.01.005

Meibom, A., Cuif, J.-P., Hillion, F., Constantz, B.R., Juillet-Leclerc, A., Dauphin, Y., Watanabe, T., Dunbar, R.B. (2004) Distribution of magnesium in coral skeleton. *Geophysical Research Letters* 31, L23306. https://doi.org/10.1029/2004GL021313

Meibom, A., Yurimoto, H., Cuif, J.-P., Domart-Coulon, I., Houlbreque, F., Constantz, B., Dauphin, Y., Tambutté, E., Tambutté, S., Allemand, D., Wooden, J., Dunbar, R. (2006) Vital effects in coral skeletal composition display strict three-dimensional control. *Geophysical Research Letters* 33, L11608. https://doi.org/10.1029/2006GL025968

Okumura, M., Kitano, Y. (1986) Coprecipitation of alkali metal ions with calcium carbonate. *Geochimica et Cosmochimica Acta* 50, 49–58. https://doi.org/10.1016/0016-7037(86)90047-5

Raiswell, R., Brimblecombe, P. (1977) The partition of manganese into aragonite between 30 and 60° C. *Chemical Geology* 19, 145–151. https://doi.org/10.1016/0009-2541(77)90011-0

Rollion-Bard, C., Blamart, D. (2015) Possible controls on Li, Na, and Mg incorporation into aragonite coral skeletons. *Chemical Geology* 396, 98–111. https://doi.org/10.1016/j.chemgeo.2014.12.011

Schleinkofer, N., Raddatz, J., Freiwald, A., Evans, D., Beuck, L., Rüggeberg, A., Liebetrau, V. (2019) Environmental and biological controls on Na/Ca ratios in scleractinian cold-water corals. *Biogeosciences* 16, 3565–3582. https://doi.org/10.5194/bg-16-3565-2019

Sinclair, D.J., Risk, M.J. (2006) A numerical model of trace-element coprecipitation in a physicochemical calcification system: Application to coral biomineralization and trace-element 'vital effects'. *Geochimica et Cosmochimica Acta* 70, 3855–3868. https://doi.org/10.1016/j.gca.2006.05.019

Standish, C.D., Milton, J.A., Page, T.M., Brown, R.M., Douglas, D., Paul, B., Schlatt, L., Foster, G.L. (2024) 2D geochemical imaging of biogenic marine carbonates using LA-TOF-ICP-MS at 1 and 2 µm pixel resolution. *Chemical Geology* 670, 122438. https://doi.org/10.1016/j.chemgeo.2024.122438